Metal attenuation processes in a landfill containing coal combustion waste: Implications for remediation

Christopher Barton, Lindy Paddock, Christopher Romanek, Sally Maharaj, and John Seaman

ABSTRACT

The 488-D Ash Basin (488-DAB) is an unlined, earthen landfill containing approximately 1 million t of dry ash and coal reject material at the U.S. Department of Energy's Savannah River Site, South Carolina. The pyritic nature of the coal rejects has resulted in the formation of acidic drainage, which has contributed to groundwater deterioration and threatened biota in adjacent wetlands. Establishment of a vegetation cover to both deplete oxygen through biological means and optimize evapotranspiration has been established as a remedial alternative for reducing acidic drainage generation in the 488-DAB. To determine the potential benefits of a cover, a series of characterization studies were conducted prior to field deployment to gain a better understanding of the metal attenuation processes and to use water quality and substrate data to evaluate the potential effectiveness of this remedial approach. The characterization study indicated that metal attenuation was primarily controlled by fluctuating redox and pH gradients associated with alternating saturated and unsaturated conditions in the basin. Based on this information, a vegetative cover could reduce the production of acid leachate over time, pending that oxygen transport to the subsurface is limited.

INTRODUCTION

The degradation of water resources from coal mining and coal combustion activities is a problem with serious environmental implications. The sulfide mineral pyrite (FeS_2) is commonly found in coal seams and their associated geologic strata and is a major contributor to the pollution problem. Acidic drainage, a low-pH

Copyright ©2005. The American Association of Petroleum Geologists/Division of Environmental Geosciences. All rights reserved.

DOI:10.1306/eg.07280404024

AUTHORS

CHRISTOPHER BARTON ~ *University of Kentucky, Department of Forestry, 203 Thomas Poe Cooper Bldg., Lexington, Kentucky 40546-0073; barton@uky.edu*

Christopher D. Barton is an assistant professor of forest hydrology and watershed management in the Department of Forestry at the University of Kentucky. As a research hydrologist with the U.S. Department of Agriculture Forest Service (1999–2003), his research focused on hydrochemical processes associated with restoration and remediation of disturbed and/or contaminated areas at the U.S. Department of Energy Savannah River Site, South Carolina.

LINDY PADDOCK ~ *University of Georgia, Savannah River Ecology Laboratory, Drawer E, Aiken, South Carolina 29802*

Lindy Paddock is a research technician III at the Savannah River Ecology Laboratory of the University of Georgia, where she manages the stable isotope laboratory. Paddock has focused her research efforts on a better understanding of the factors that influence the chemical evolution of pore fluids in sulfidic materials, including coal deposits.

CHRISTOPHER ROMANEK ~ *University of Georgia, Savannah River Ecology Laboratory, Drawer E, Aiken, South Carolina 29802; present address: Department of Geology, University of Georgia, Athens, Georgia 30602*

Christopher Romanek is an associate professor of geology and associate research professor at the Savannah River Ecology Laboratory of the University of Georgia. His primary area of research is low-temperature geochemistry, with an emphasis on the stable isotope systematics of carbonate minerals. In addition, he has studied the effects of microorganisms on the remediation of acid mine drainage in wetland systems.

SALLY MAHARAJ ~ *University of Kentucky, Department of Forestry, 203 Thomas Poe Cooper Bldg., Lexington, Kentucky, 40546-0073*

Sally Maharaj is a graduate student in the Department of Geology at the University of Kentucky. Maharaj interned at the Savannah River

Site as an undergraduate with the South Carolina State University and the Savannah River Environmental Sciences Field Station during the summers of 2002 and 2003.

JOHN SEAMAN ~ *University of Georgia, Savannah River Ecology Laboratory, Drawer E, Aiken, South Carolina 29802*

John C. Seaman is an associate research professor with the Savannah River Ecology Laboratory, located on the Savannah River Site and operated for the Department of Energy by the University of Georgia. Seaman received his B.S. (1987) and M.S. (1990) degrees from Texas A&M University in agronomy and soil science, respectively, and his Ph.D. (1994) in environmental soil science from the University of Georgia.

ACKNOWLEDGEMENTS

This work was funded in part by the U.S. Department of Energy–Savannah River Operations Office through the U.S. Forest Service–Savannah River (Interagency Agreement DE-IA09-00SR22188) and the Savannah River Ecology Laboratory through the University of Georgia Research Foundation, Inc. (Financial Assistance Award DE-FC09-96SR18546). Support was also provided by the U.S. Forest Service-Southern Research Station, Center for Forested Wetlands Research, and the Environmental Research and Training Laboratory at the University of Kentucky.

water enriched in iron, aluminum, sulfate, and trace elements, is formed when pyrite is exposed to the oxidizing forces of air and water. The oxidation and subsequent formation of acidic drainage is a complex process involving hydrolysis, redox, and microbial reactions (Nordstrom, 1982). The general stoichiometry can be described by the following reaction:

$$FeS_{2(s)} + 3.757O_2 + 3.5H_2O \rightarrow Fe(OH)_{3(s)} + 2H_2SO_4$$

where iron sulfide and other mixed-metal sulfides decompose upon exposure to the atmosphere, producing sulfuric acid and insoluble ferric iron hydroxide from hydrolysis (Bigham et al., 1992). As the sulfuric acid interacts with materials in the surrounding environment (coal, ash, soil, etc.), dissolution of minerals and mobilization of metals and trace elements found in the solids may ensue.

The ferric iron precipitate and associated acidity are generally considered the principal causes for the degradation of water bodies receiving acidic drainage and for the endangerment of aquatic species that reside within. The mineralogy of precipitates forming in acidic drainage systems are generally referred to as amorphous ferric hydroxides (Stumm and Morgan, 1981); however, recent studies have focused on many discrete minerals associated with these systems (e.g., ferrihydrite [$5Fe_2O_3 \cdot 9H_2O$], jarosite [$KFe_3(OH)$], goethite [α-FeOOH], and/or lepidocrocite [γ-FeOOH]) that may have significant implications toward understanding metal attenuation processes in these acidic environments (Barton and Karathanasis, 1998, and references within). Environments with alternating abiotic and biotic substrates exhibit a variety of pH and redox conditions, and chemical speciation under the varying conditions is consequently influenced. Lazaroff et al. (1982) reported that low-pH acidic drainage precipitates formed under abiotic conditions contained goethite and some hydrated Fe(III) sulfates, whereas those formed under biotic conditions and in the presence of *Thiobacillus ferrooxidans* bacterium were dominated by amorphous hydrated Fe(III) sulfates. Under anaerobic conditions and in the presence of organic carbon, however, iron oxide and oxyhydroxide formation may be inhibited due the formation of organometal complexes (Karathanasis and Thompson, 1995). As such, metal attenuation in acidic drainage-forming substrates is influenced by redox conditions, organic matter content, and also by environmental conditions that may affect the microbial communities (i.e., temperature and pH).

Several innovative techniques have been proposed to reduce acidic drainage generation by limiting the exposure of pyrite to air and water. A dry cover is one such technology that uses a layer of soil, compost, or other organic material (peat, hay, straw, and sawdust) above mining waste to deplete oxygen through bacterial consumption (Pierce et al., 1994). The organic waste may also inhibit oxidation by removal of Fe^{3+} from solution through complexation and the formation of pyrite–Fe^{2+}–humate complexes (Evangelou, 1995). Changes in the particle-size distribution of the cover over that of the mining waste may also be engineered to enhance water

storativity. As such, water percolation through the waste and exposure to the pyrite could be decreased. The use of vegetation may also be included in the design to aid in the removal of water through evapotranspiration (Dobson and Moffat, 1995). The net effect of these techniques is to cut off the oxygen source and to stabilize sediments on the site.

Establishment of a vegetation cover to both deplete oxygen through biological means and optimize evapotranspiration was proposed as a remedial alternative for reducing acidic drainage generation in the 488-D Ash Basin (488-DAB) at the U.S. Department of Energy's Savannah River Site, South Carolina. Prior to the field deployment, mechanisms controlling the oxidation of pyrite and metal attenuation in the landfill were not well understood. Hence, a series of characterization studies were conducted to examine these processes and to evaluate the potential effectiveness of the proposed remedial approach.

MATERIALS AND METHODS

Site Description and Background

The 488-DAB is an unlined, earthen containment basin located on the Savannah River Site, South Carolina, that received sluiced fly ash, dry fly ash, and coal reject material from the early 1950s to the mid 1990s (Figure 1). The 488-DAB is about 550 × 180 × 5.5 m (1804 × 590 × 18 ft) in size and contains about 5.4×10^5 m^3 (1.9×10^7 ft^3) of waste material. The basin was constructed on the existing land surface at about 35 m (114 ft) (mean sea level) and is about 9 m (29 ft) above the Savannah River. The present surface of the basin slopes gently to the west and is filled with waste, except in the far western reach where surface waters collect during rainfall events.

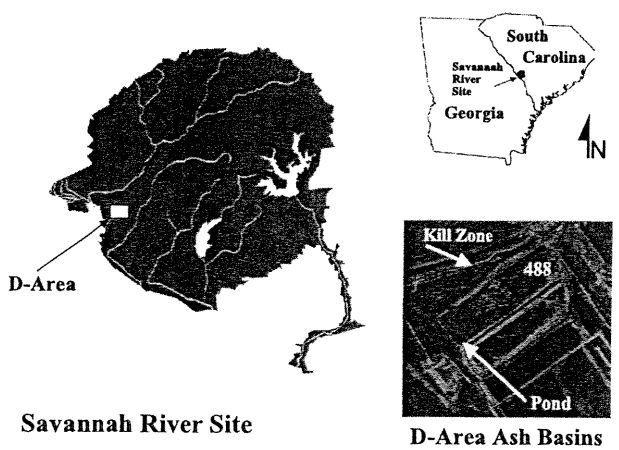

Figure 1. D-Area power plant and vicinity on the Savannah River Site, South Carolina.

The extent of water-saturated material in 488-DAB is not known, nor if any communication exists between basin waste and the local water table. Based on limited soil borings, the waste seems to be variably saturated, having both wet and dry zones that vary with depth. The source of this water may be meteoric infiltration or lateral groundwater flow from adjacent basins. Hydraulic anisotropies may have been created when various materials were introduced to the basin. Alternatively, postdepositional features such as diagenetic hard pans may have developed as materials weathered, creating local anisotropies

Sample Collection

A 2 × 1 × 1-m (6.6 × 3.3 × 3.3-ft) deep trench was excavated in the center of 488-DAB to retrieve material for the characterization study. Six horizons were noted in a cross section of the trench; of these, a coal rubble zone (A) and fly ash residue zone (D) best represented the character of the waste and were chosen for additional study. In the field, zone A consisted of poorly sorted, pebble-sized pieces of coal and pyrite, whereas zone D contained a relatively uniform fine-grained material. Approximately 1 m^3 (35 ft^3) of material was shoveled from zone A and D into individual plastic bags and subsequently placed inside large plastic containers to minimize atmospheric interaction. The containers were transported to the laboratory where subsamples were collected for thin sectioning. Additional subsamples were dried and sieved to less than 2 mm (0.08 in.) then sequentially extracted to determine the soluble, exchangeable, organically bound, poorly crystalline, crystalline, and residual forms of metal bound to the substrate. The metal fractionation method used was modified from those described by Henrot and Weider (1990) and McDaniel and Buol (1991) as outlined in Table 1.

Surface water samples were collected biweekly from three locations during the period June 1999 to September 2000 and again in June of 2001 and 2002. The sample locations were (1) ponded area at the west end of the basin, (2) pipe leak at the west berm of the basin, and (3) the stressed and dead vegetation area (kill zone) adjacent to the north berm (Figure 1). Subsurface water samples from the basin were collected on a quarterly basis using lysimeters. Suction (tension)

Table 1. Sequential Extraction Procedure for 488-DAB Material

Step	Fraction	Solution	Soil (g)	Solution (mL)	Conditions
1	water soluble	DDI water	1.0	10	shake 30 min
2	exchangeable	1 M KNO_3	1.0	25	shake 16 hr (overnight)
3	organically bound	0.1 M $Na_4P_2O_7$	1.0	15	shake 16 hr (overnight)
4	poorly crystalline	0.2 M $(NH_4)_2C_2O_4H_2O$; 0.2 M $H_2C_2O_4$ (pH 3.0)	1.0	15	shake 4 hr in the dark
5	crystalline	CBD: 0.3 M $Na_3C_6H_5O_7 \cdot 2H_2O$; 0.1 M $NaHCO_3$; 1 g $Na_2S_2O_3$	1.0	15	heat at 80°C in a water bath for 1 hr; stir occasionally
6	residual	(1:4) HCl; (1:1) HNO_3	1.0	10; 4	reflux on hot plate for 30 min (do not boil)

DDI = distilled deionized water; CBD = citrate-bicarbonate-dithionite.

lysimeters at 200 cm (78 in.) were installed at three locations on the basin. Lysimeter placement involved coring a 5-cm (1.9-in.)-diameter hole to the desired depth using a bucket auger. A slurry was formed from a portion of the excavated soil and then poured into the hole where the lysimeter rests, such that the porous ceramic cup on the sampler is completely surrounded by the mixture. The remaining area above the slurry was backfilled with the original soil and firmly tamped to prevent short circuiting. A plug of bentonite clay was placed around the lysimeter to further prevent preferential flow of water in the backfilled area. Once installed, a vacuum of 60 cbar was applied to the lysimeter using a hand vacuum pump. A stopper assembly equipped with a neoprene tube and pinch clamp was used to contain the applied vacuum. Water samples were extracted from the lysimeters by disconnecting the stopper assembly and pumping the collected water into polyethylene bottles.

Column Experiment

Flowthrough columns were made using clear polyvinyl chloride (PVC) pipe of approximately 15 cm (6 in.) in diameter and 25 cm (9.8 in.) in length (~4500 cm^3; ~274 $in.^3$). Attached to the ends of each cylinder were PVC plates that contained individual ports for influent and effluent flow of both gasses and liquids. Columns were flushed with fluid from the bottom up to minimize air-filled void space and from top to bottom with gas to facilitate the expulsion of liquid and to accelerate the drying process. Waste material from the selected horizons was packed in the columns. Nylon screens (600-mesh) were attached at each end of a column to prevent mass loss. Gas-equilibrated water was pumped independently into the columns from a common reservoir at 2.5 mL min^{-1}. Nonpotable groundwater pumped from a local artesian aquifer was stored in 50-L carboys and pre-equilibrated to the appropriate temperature and gaseous conditions before being pumped into the columns.

Four experimental runs were conducted sequentially; each run consisted of four independent columns that were leached for approximately 35 days. In each run, two columns contained zone A material, and two columns contained zone D material. One column from each zone was flushed continually with fluid, whereas the others experienced a periodic wetting (5 days) and drying (2 days) cycle flow regime. Column experiments were conducted at two different temperatures, 12.7 and 29.4°C, to simulate winter and summer soil temperatures, respectively. Maintenance of the experimental conditions was achieved by housing the entire column setup, including gas and liquid reservoirs, in a large environmental chamber. The treatment sequence for the experimental runs was (1) O_2-equilibrated fluid at 12.7°C (run 1), (2) N_2-equilibrated fluid at 12.7°C (run 2), (3) N_2-equilibrated fluid at 29.4°C (run 3), and (4) O_2-equilibrated fluid at 29.4°C (run 4). When a column experiment was initiated, effluent was collected every 4 hr for the first 48 hr and daily thereafter. During each sampling event, effluent pH, oxidation-reduction potential (E_h), temperature, and electrical conductivity (EC) were recorded, the measurements of total Fe and Fe^{2+} were performed (HACH® test kit), and fluid samples were collected and preserved for laboratory analysis.

Analytical Methods

Field measurement of pH and EC was performed using a HYDROLAB®. Water samples were packed in ice and transported to the laboratory. Samples were

filtered (0.45 μm), preserved as deemed necessary according to procedures in the Standard Method for the Examination of Water and Wastewater (American Public Health Association, 1989), and stored in a refrigerator at 4°C until analyzed. Measurements of pH, E_h, temperature, and EC in the environmental chamber were made using hand-held meter and probes (Hanna, Orion). Calibration checks were performed on all probes once per week for quality control. Elemental analysis of field samples and column eluents were performed by inductively coupled plasma–optical emission spectroscopy (ICP-OES) analyses on a Perkin-Elmer Optima 4500DV Optical Emission Spectrometer. Total Fe, Fe^{2+}, and sulfate analysis were conducted using HACH® test kits and a DR/890 Colorimeter.

The XRD analyses were conducted on powder mounts of zone A and D materials using an x-ray diffraction (XRD) diffractometer (X2 Advanced Diffraction System, Scintag Inc.) with Co Kα radiation. A TGA 2950 thermogravimetric analyzer (TA Instruments, New Castle, Delaware) was used for thermogravimetric and differential thermogravimetric characterizations.

Analysis of the various soil fractions was performed by inductively coupled plasma–mass spectrometry or optical emission spectrometry (ICP-MS or ICP-OES). An extraction for total recoverable elements was performed on separate samples using the HNO_3-HCl-microwave-based digestion method [U.S. Environmental Protection Agency (USEPA), 1996, method 200.2] followed by ICP-MS and ICP-OES. Quality assurance-quality control protocols were followed for all analytical procedures as outlined in USEPA (1994) method 6020.

RESULTS AND DISCUSSION

Surface Water and Interstitial Solution Composition

Biweekly water samples were collected from three locations on and adjacent to the 488-DAB from June 1999 to September 2000 and again in June 2001 and 2002. Average pH values from the three locations were consistently in the 2.5–3.5 range (Table 2). Samples

Table 2. Average Surface and Vadose Water-Quality Characteristics from the 488-DAB*

Parameter	Surface Pond**	Pipe Leak**	Kill Zone**	200-cm (78-in.) Lysimeter***
n	42	52	56	17
pH	2.71 (0.23)	3.16 (0.29)	2.84 (0.23)	2.49 (0.64)
Al (mg L^{-1})	82.9 (112.7)	153.3 (93.5)	29.7 (66.3)	831.5 (740.2)
As (mg L^{-1})	0.22 (0.65)	BDL	BDL	2.80 (5.65)
Ca (mg L^{-1})	100.4 (42.8)	123.6 (30.1)	53.6 (60.7)	350.7 (133.8)
Cd (mg L^{-1})	BDL	BDL	BDL	0.92 (0.58)
Cr (mg L^{-1})	0.04 (0.04)	0.02 (0.03)	BDL	0.48 (0.79)
Cu (mg L^{-1})	0.15 (0.15)	0.07 (0.04)	BDL	7.49 (14.3)
Fe (mg L^{-1})	181.3 (245.1)	213.8 (72.3)	57.0 (58.1)	7460.1 (3971.1)
K (mg L^{-1})	2.64 (2.38)	12.8 (4.6)	6.28 (4.21)	BDL
Mg (mg L^{-1})	33.4 (72.5)	43.7 (26.8)	23.9 (39.8)	431.1 (195.2)
Mn (mg L^{-1})	1.56 (2.83)	2.14 (0.66)	1.95 (2.25)	41.3 (16.1)
Na (mg L^{-1})	5.83 (9.22)	9.21 (4.69)	25.1 (17.8)	31.2 (16.6)
Ni (mg L^{-1})	0.15 (0.26)	0.31 (0.09)	0.05 (0.06)	BDL
Se (mg L^{-1})	BDL	0.01 (0.01)	BDL	BDL
Zn (mg L^{-1})	0.29 (0.29)	0.48 (0.18)	0.18 (0.13)	13.5 (14.7)
SO_4 (g L^{-1})	1.41 (1.43)	1.62 (0.43)	0.57 (0.51)	4.80 (1.98)
Ba (mg L^{-1})	0.04 (0.04)	0.04 (0.03)	0.05 (0.05)	
B (mg L^{-1})	0.27 (0.13)	0.47 (0.34)	0.31 (0.05)	
Fe (II) (%)	11.7 (15.3)	83.5 (16.4)	40.0 (20.5)	

BDL = below detection limit.
*Standard deviations are in parenthesis.
**Surface water samples collected biweekly from July 1999 to September 2000 and in June 2001 and 2002.
***Vadose samples collected quarterly from three lysimeters at 200-cm (78-in.) depth during the period April 2001–October 2002.

from the surface pond and seepage from the ponded area (pipe leak) contained high concentrations of Al, Fe, and sulfate, which is characteristic of acidic drainage from mining sites and coal combustion waste areas (Evangelou, 1995). Samples collected from the kill zone (Figure 1) also exhibited these constituents but at a slightly lower concentration. An outfall from the D-Area powerhouse contributed uncontaminated water to the kill zone area and likely produced a dilution effect. Iron in the surface pond was primarily in the ferric (Fe^{3+}) oxidation state, whereas ferrous iron (Fe^{2+}) dominated samples from the pipe leak. The iron oxidation provides information on the origin of the water. Drainage in the pond likely originates from surface oxidation of pyrite and subsequent runoff across the gently sloping surface of the basin. High compaction of the basin sediments likely promotes these actions by limiting infiltration and maximizing contact of the basin material with oxygenated precipitation. The lowest point in the surface topography of the basin is the ponded area at the west end. Once drainage was collected in that location, seepage and leakage occurs through the sediment and ultimately through the berm. As the water slowly perked through the basin sediments, oxygen diffusion was likely reduced, and microbial consumption of oxygen increased. Consequently, Fe^{3+} was reduced to Fe^{2+}, and a slight rise in pH occurred. As conditions became more anaerobic, the formation of metal sulfides and alkalinity through bacterially mediated sulfate reduction likely occurred in a fashion similar to that described in constructed wetlands treating acidic drainage (Barton and Karathanasis, 1999).

Water samples collected from three lysimeters at a depth of 200 cm (78 in.) exhibited a lower pH and higher elemental composition than the surface waters (Table 2). Not only were the concentrations higher in the lysimeters, but levels were also generally an order of magnitude greater for most parameters analyzed. Given the low permeability of the substrate material and high pyrite content of the substrate, the high concentrations were expected. Water likely stayed in close contact with the reactive material in this zone for an extended period of time, which allowed for maximum oxidation of the sulfide materials and dissolution of evaporative salts. As the pore water slowly moved through the sediments, oxygen consumption increased, pH rose, and metals likely precipitated as discrete minerals in the substrate. Thus, a significant amount of filtering may have occurred in the basin prior to release through the berm or below grade.

Mineralogy

Using XRD, thermal analysis, and thin sections of material from zones A and D, Barton et al. (2003) found that zone A contained large clasts of coal and detrital pyrite, whereas zone D predominantly contained fine-grained material that was identified as either detrital or authigenic pyrite. The fluctuating saturated and unsaturated conditions in the field promoted incongruent precipitation and dissolution of minerals on the basin's surface. During dry periods of the summer, yellow efflorescences erupted from below the surface and were a common superficial feature on the basin. In addition, white globules consisting of a hard inner shell and soft outer coating with a powder consistency were abundant in the upper 1 cm (0.4 in.) of the surface horizon. X-ray diffraction patterns of the yellow efflorescence were consistent with those of the iron sulfate mineral coquimbite [$Fe_2(SO_4)_3 \cdot 9H_2O$]. The precipitation of iron sulfate minerals is a common product of an evaporative system that has accumulated dissolved species from pyrite oxidation (Bigham and Nordstrom, 2000). As noted by Jambor et al. (2000), the subsequent dissolution of these salts during rain events represents an additional source of acidity and a major contributor to the contaminant pool of these systems and adjacent environments. Minerals associated with the white globular material were identified by XRD as gypsum ($CaSO_4 \cdot 2H_2O$) and calcite ($CaCO_3$). Apparently, the acidic conditions of the basin have contributed to the dissolution of limestone particles that were comingled in the waste material.

The XRD patterns of basin material collected from zones A and D exhibited a very similar array of peaks and suggested the presence of quartz, pyrite, and possibly goethite (α-FeOOH). Material from zone A also displayed weak reflections indicative of basaluminite [$Al(SO_4)(OH)_{10}$]. Insoluble aluminum hydroxysulfates may precipitate from acid sulfate solutions when buffered to a relatively high pH by carbonate materials; however, a pH near 5.0 must be achieved for this to occur (pK_1 for Al hydrolysis is 5.0; Nordstrom and May, 1996). Although the presence of calcite was verified in this zone, samples analyzed for pH sparsely exceeded a value greater than 2.5. It is possible that such minerals formed in the local environment when pH was buffer by a release of alkalinity. Thermogravimetric analysis of zone A material suggested the presence of gypsum, pyrite, calcite, a poorly crystalline goethite, lepidocrocite (γ-FeOOH), or akaganeite, and/or an Al-hydroxide mineral. Material from zone D showed

deflections that were consistent with that of goethite and pyrite.

Based on the results, Barton et al. (2003) suggested that materials in the upper part of the basin were enriched to some extent with carbonate materials, whereas subsurface zones were primarily dominated with pyrite and secondary precipitates that resulted from its oxidation. Gypsum precipitation was indicated to be a surface phenomenon caused by the relative abundance of carbonates in that zone. In addition, the presence of Al hydroxides in zone A is also likely a by-product of the dissolution of calcite and alkalinity release on the surface. A conceptual mineralogical model of the basin is presented in Figure 2.

Element Fractionation

Sequential extraction of zone A materials revealed that the water-soluble and exchangeable bound fractions contained minimal Fe concentrations (Figure 3). Approximately 70% of the Fe in zone A was extracted in the poorly crystalline fraction, with a slight contribution (<10%) from the organically bound fraction. Substrates with little organically bound iron can attribute the poorly crystalline fraction to ferrihydrite, which is ammonium oxalate soluble (Schwertmann and Taylor, 1989). In the deeper zone D sediments, a large reduction in the organically bound fraction and increase in the crystalline fraction was observed (Figure 4). The loss of the organically bound phase is likely the result of lower organic matter concentrations in the deeper zone. The increase in citrate-bicarbonate-dithionite-extracted Fe in the deeper zone is likely linked to the elution of minerals, such as goethite, hematite, and lepidocrocite, which are oxalate insoluble.

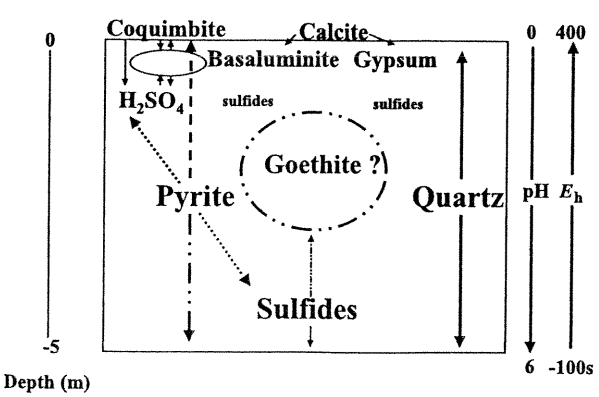

Figure 2. Conceptual model for mineral phase location in the 488-DAB as influenced by pH-E_h gradient and depth. The presence of each phase was confirmed using x-ray diffraction, thermal analysis, thin-section microscopy, or by geochemical speciation.

Manganese fractionation exhibited substantially different patterns than those observed for Fe (Figures 3, 4). Exchangeable forms of Mn dominated in zone A material, whereas the deeper material was dominated by the poorly crystalline Mn fraction. High exchangeable Mn fractions have been noted elsewhere in systems that are influenced by coal combustion waste and acidic drainage (Weider et al., 1990; Anderson et al., 1991). The replacement of exchangeable fractions by poorly crystalline forms in the deeper zone is probably the result of an increase in pH. Although a pH > 8.0 is generally needed for Mn precipitation, Mn in areas with high Fe concentrations may undergo coprecipitation with Fe at much lower pH levels (Stumm and Morgan, 1981). It has also been shown that Mn^{2+} can be removed by adsorption to reactive surfaces of crystalline Fe minerals at low pH values. Thus, the poorly crystalline and crystalline Mn phases may be controlled by the type and amount of Fe present in the sample.

In both zones, Al and As were primarily observed in the poorly crystalline phase with a smaller amount found in the organic phase (Figures 3, 4). The fractionation patterns of Al and As are very similar to that of Fe, suggesting that their solubility may be controlled by an Fe-dominated mineral or precipitate. Zinc was found in both the organic and poorly crystalline fractions in appreciable quantities. It has been shown that Zn is retained on oxyhydroxides by surface complexation and, thus, can be solubilized through mineral dissolution (Calvet and Bourgeois, 1990). As with Al and As, the primary control on Zn solubility may be explained by the formation and dissolution of secondary amorphous Fe precipitates in the basin. The organically bound Zn phase showed a decrease with depth from 35 to 18%. Zinc has been shown to have a weak association with organic matter and is readily released during this extraction phase (Narwal et al., 1999).

Selenium was limited to the crystalline and residual phases in both zones (Figures 3, 4). This partitioning behavior is in stark contrast with the other elements described earlier and implies that Se is strongly associated with either a primary mineral or a silicate. As such, the mobility and potential for bioavailability of Se is low as compared to that of the other elements.

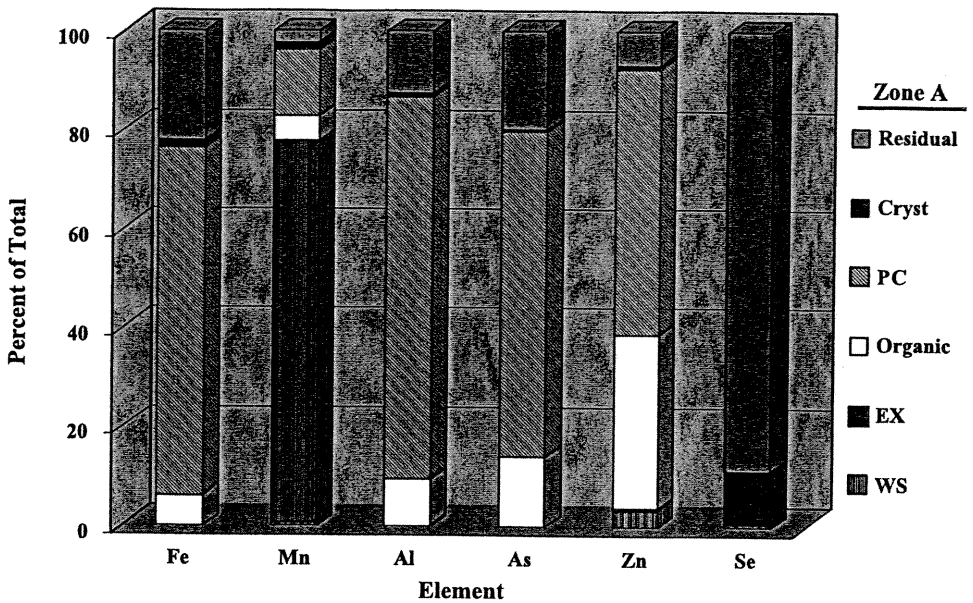

Figure 3. Distribution of Fe, Mn, Al, As, Zn, and Se in sequentially extracted sediments from zone A of the 488-DAB. Elements were separated into water-soluble (WS), exchangeable (EX), organically bound (Organic), poorly crystalline (PC), crystalline (Cryst), and residual (Residual) fractions.

Column Eluents

An inverse correlation was observed between E_h and pH for all four experimental runs, and this relationship is similar to that noted elsewhere for acid mine drainage (Garrels and Christ, 1990; Faure, 1991). In general, pH increased from about 1.0 to 6.0 over the first 2 weeks and then remained relatively constant thereafter (Figure 5). Similar low pH values (pH $\sim$ 1 or lower) have been observed in sulfide-rich tailings impoundments and mine waste sites that have been exposed to atmospheric conditions for long periods of time (Blowes et al., 1991; Nordstrom et al., 2000). The relationship between E_h and pH was consistent (r^2 = 0.78) both within columns of an experimental run (e.g., among flow regimes for both the coal rubble and fly ash residues) and among experimental runs (e.g., for different fluid compositions and temperatures). This observation suggests that the basic chemical mechanism responsible for the production of column effluent was similar among treatments. In addition, the closeness of the curve fit between runs may suggest that the

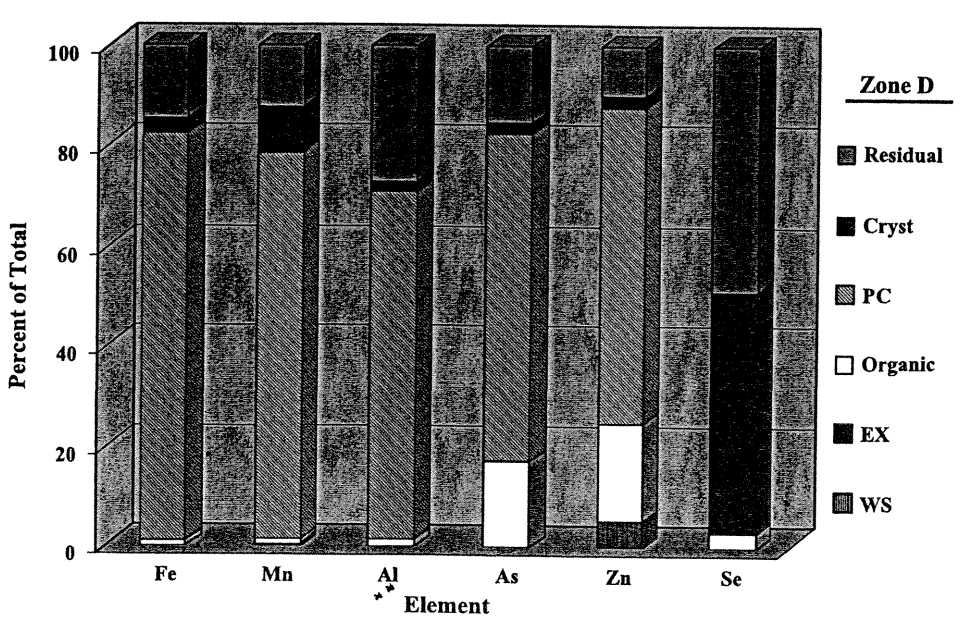

Figure 4. Distribution of Fe, Mn, Al, As, Zn, and Se in sequentially extracted sediments from zone D of the 488-DAB. Elements were separated into water-soluble (WS), exchangeable (EX), organically bound (Organic), poorly crystalline (PC), crystalline (Cryst), and residual (Residual) fractions.

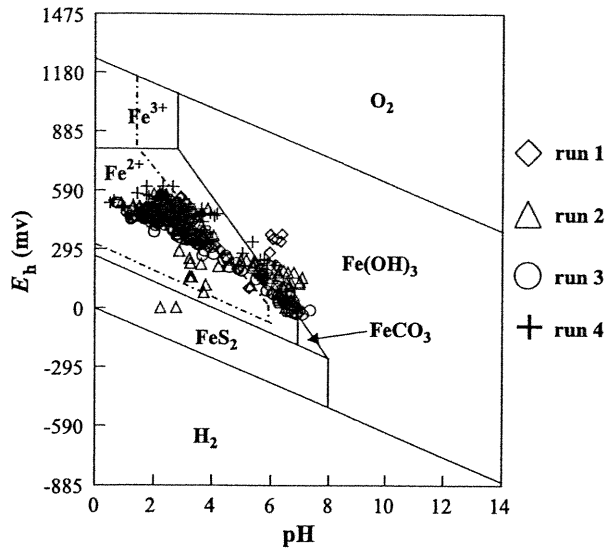

Figure 5. E_h–pH diagram for the stability of pyrite, $Fe(OH)_3$, and $FeCO_3$ in water at 25°C and 1 atmosphere of pressure. Eluents from the various column experiments are superimposed on the stability diagram. The activity of $SO_4^{2-} = 10^{-3}$ M, and $Fe^{2+} = 10^{-4}$ M. Siderite ($FeCO_3$) was assumed to have a K_{sp} of $10^{-10.5}$. The dashed line represents the hypothetical solid-solution boundary for Fe(aq) = 10^{-2} mol/kg, which is consistent with interstitial solution concentrations from lysimeters and initial column eluents. The figure is modified after Evangelou (1995) and Nordstrom (1982).

driver for pyrite oxidation in these sediments is one of a physicochemical instead of a biological nature. Ferric iron may act as an electron acceptor and contribute to acid production through hydrolysis and/or as a direct mechanism for pyrite oxidation. Further examination of Figure 5 reveals two dominating clusters of points; one in the pH 2–3 range with E_h values between 400 and 500 mv, and another in the pH 5–7 range with E_h values less than 200 mv. The clusters may represent the transition of iron from the soluble Fe^{2+} valence state to an insoluble Fe^{3+} precipitate. With the removal of ferric iron from the system (via precipitation), acid generation and potential pyrite oxidation is lowered, and waters make the transition from acidic to circumneutral.

In the latter stages of the column experiment, effluents appeared to be at saturation with an iron-hydroxide mineral (Figure 5). Using the equilibrium geochemical speciation model MINTEQA2 (Allison et al., 1990), eluent saturation indices (log Q/K, where Q = ion activity product and K = solubility product constant) were examined to identify the potential mineral phases. Results from the modeling exercise indicated that the eluents collected during the final week of leaching were at or near equilibrium with ferrihydrite, goethite, and lepidocrocite. Conversely, saturation indices for pyrite, jarosite, and coquimbite were negative, which is indicative of an undersaturated state. As such, maintenance of the system in a more reducing condition than the present (about <300 mv) may be an essential factor for the control of pyrite oxidation and iron mobility in these sediments.

CONCLUSIONS

In an effort to evaluate remedial options for an abandoned fly ash and a reject coal landfill, characterization of the geochemistry of the waste material and associated leachate was examined. Information was generated using acidic drainage sampled at various locations on and adjacent to the basin and from materials located on the surface of the landfill, primarily coal rubble and fly ash residue. The water chemistry exhibited characteristics common to acidic drainage deriving from mine and coal combustion waste sites; low pH, high Fe, Al, SO_4, and trace-element concentrations. Lysimeter samples collected in the vadose zone, however, were more concentrated with respect to these elements over that observed in surface waters, which suggest that water was in close contact with reactive materials in the basin for an extended period of time. As the pore water slowly moved through the basin sediments and into the saturated zone, pH rose, and metals likely precipitated as discrete minerals in the substrate. Thus, some amelioration of the water may have occurred in the basin prior to release through the berm or below grade because of changes in saturation and redox conditions. Characterization of sediment samples collected from the surface of the basin revealed the presence of large clasts of coal and detrital pyrite, secondary iron and aluminum precipitates, and evaporative iron sulfate and calcium sulfate salts, which formed from the weathering of pyrite and dissolution of carbonates. The iron sulfate salts (coquimbite) represent a significant source of acidity on the landfill. The deeper fly ash material contained authigenic pyrite framboids that were likely formed through the weathering of the overlying detrital pyrite fragments and secondary iron precipitates. Sequential extraction performed on the sediments indicated that Fe was primarily found in the poorly crystalline and crystalline fractions. Elemental fractionation for Al, As, Zn, and zone D Mn were similar to that of Fe,

suggesting that their solubility may be controlled by an Fe-dominated mineral or precipitate. As such, mobility of these species is likely controlled by precipitation and resolubilization of Fe under the varying redox and pH environments of the basin. Surficial Mn fractionation, however, was predominantly in the exchangeable fraction. Selenium was limited to the crystalline and residual phases, which suggest that its mobility or availability to plants is low. A linear correlation was observed between E_h and pH during a leaching experiment using basin materials. In general, pH increased over time as redox conditions became more anaerobic, and a subsequent decrease in Fe was observed as a result of precipitation. This finding suggests that acid production on the basin may be maintained by poising the iron redox couple at a level favoring the ferrous state (about <300 mv). As such, the design of a vegetative cover on the basin should consider methods that would limit surface oxidation via organic matter incorporation (litter or compost) or the installation of an impermeable barrier.

REFERENCES CITED

Allison, J. D., D. S. Brown, and K. J. Novo-Gradac, 1990, MINTEQA2/PRODEFA2, a geochemical assessment method for environmental systems, version 3.0 user manual: Athens, Georgia, U. S. Environmental Protection Agency Environmental Research Laboratory, 106 p.

American Public Health Association, 1989, Standard methods for the examination of water and wastewater, 17th ed.: Washington, D.C., American Public Health Association, 949 p.

Anderson, M. A., P. M. Bertsch, S. B. Feldman, and L. W. Zelazny, 1991, Interactions of acidic metal-rich coal pile runoff with a subsoil: Environmental Science and Technology, v. 25, p. 2038–2046.

Barton, C. D., and A. D. Karathanasis, 1998, Aerobic and anaerobic metal attenuation processes in a constructed wetland treating acid mine drainage: Environmental Geosciences, v. 5, no. 2, p. 43–56.

Barton, C. D., and A. D. Karathanasis, 1999, Renovation of a failed constructed wetland treating high metal load acid mine drainage: Environmental Geology, v. 39, no. 1, p. 39–50.

Barton, C. D., L. Paddock, C. Romanek, and J. Seaman, 2003, Geochemistry of an abandoned landfill containing coal combustion waste: Implications for remediation, *in* K. Sajwan, A. K. Alva, and R. F. Keefer, eds., Chemistry of Trace Elements in Fly Ash: New York, Kluwer Academic Publishers, p. 105–141.

Bigham, J. M., and D. K. Nordstrom, 2000, Iron and aluminum hydroxysulfates from acid sulfate waters, *in* C. N. Alpers, J. L. Jambor, and D. K. Nordstrom, eds., Reviews in mineralogy and geochemistry: Sulfate minerals: Washington, D.C., Mineralogical Society of America, v. 40, p. 351–393.

Bigham, J. M., U. Schwertmann, and L. Carlson, 1992, Mineralogy of precipitates formed by the biogeochemical oxidation of Fe(II) in mine drainage, *in* H. C. W. Skinner and R. W. Fitzpatric, eds., Biomineralization: Cremlingen-Destedt, Germany, Catena Verlag, p. 219–232.

Blowes, D. W., E. J. Reardon, J. L. Jambor, and J. A. Cherry, 1991, The formulation and potential importance of cemented layers in inactive sulfide mine tailings: Geochimica et Cosmochimica Acta, v. 55, p. 965–978.

Calvet, R., and S. Bourgeois, 1990, Some experiments on extraction of heavy metals present in soils: International Journal of Environmental Analytical Chemistry, v. 39, p. 31–45.

Dobson, M. C., and A. J. Moffat, 1995, A re-evaluation of objections to tree planting on contaminated landfills: Waste Management and Research, v. 13, p. 579–600.

Evangelou, V. P., 1995, Pyrite oxidation and its control: Boca Raton, CRC Press, 293 p.

Faure, G., 1991, Principles and applications of inorganic chemistry: New York, Macmillan Publishing Co, 626 p.

Garrels, R. M., and C. L. Christ, 1990, Solutions, minerals, and equilibria: Boston, Jones and Bartlette Publishers, Inc, 450 p.

Henrot, J., and R. K. Weider, 1990, Processes of iron and manganese retention in laboratory peat microcosms subjected to acid mine drainage: Journal of Environmental Quality, v. 19, p. 312–320.

Jambor, J. L., D. K. Nordstrom, and C. N. Alpers, 2000, Metal-sulfate salts from sulfide mineral oxidation, *in* C. N. Alpers, J. L. Jambor, and D. K. Nordstrom, eds., Reviews in mineralogy and geochemistry: Sulfate minerals: Washington, D.C., Mineralogical Society of America, v. 40, p. 305–350.

Karathanasis, A. D., and Y. L. Thompson, 1995, Mineralogy of iron precipitates in a constructed acid mine drainage wetland: Soil Science Society of America Journal, v. 54, p. 1773–1781.

Lazaroff, N., W. Sigal, and A. Wasserman, 1982, Iron oxidation and precipitation of ferric hydroxysulfates by resting *Thiobacillus ferrooxidans* cells: Applied Environmental Microbiology, v. 43, p. 924–938.

McDaniel, P. A., and S. W. Buol, 1991, Manganese distributions in acids soils of the North Carolina Piedmont: Soil Science Society of America Journal, v. 55, p. 152–158.

Narwal, R. P., B. R. Singh, and B. Salbu, 1999, Association of cadmium, zinc, copper, and nickel with components in naturally heavy metal rich soils studied by parallel and sequential extraction: Communications in Soil Science and Plant Analysis, v. 30, p. 1209–1230.

Nordstrom, D. K., 1982, Aqueous pyrite oxidation and the consequent formation of secondary iron minerals, *in* J. A. Kittrick, D. S. Fanning, and L. R. Hossner, eds., Acid sulfate weathering: Soil Science Society of America Special Publication 17, p. 37–56.

Nordstrom, D. K., and H. M. May, 1996, Aqueous equilibrium data for mononuclear aluminum species, *in* G. Sposito, ed., The environmental chemistry of aluminum, 2d ed.: Boca Raton, Florida, CRC Press–Lewis Publishers, p. 39–80.

Nordstrom, D. K., C. N. Alpers, C. J. Ptacek, and D. W. Blowes, 2000, Negative pH and extremely acidic mine waters from Iron Mountain, California: Environmental Science and Technology, v. 34, p. 254–258.

Pierce, W. G., B. Belzile, M. E. Wiseman, and K. Winterhalder, 1994, Proceedings of the International Land Reclamation and Mine Drainage Conference, SP06B-94: Pittsburgh, Pennsylvania, U.S. Department of the Interior, v. 2, p.148–157.

Schwertmann, U., and R. M. Taylor, 1989, Iron oxides, *in* J. B. Dixon and S. B. Weed, eds., Minerals in the soil environment, 2d ed.: Madison, Wisconsin, Soil Science Society of America, p. 379–438.

Stumm, W., and J. J. Morgan, 1981, Aquatic chemistry, 2d ed.: New York, J. Wiley & Sons, 780 p.

USEPA, 1994, Inductively coupled plasma-mass spectrometry, method 6020, Rev. 0, *in* SW-846: Test methods for evaluating solid waste, physical/chemical methods: Washington, D.C., U.S. Environmental Protection Agency Office of Solid Waste, p. 6020-1–6020-18.

USEPA, 1996, Microwave assisted acid digestion of siliceous and organically based matrices, method 3052, Rev 0, *in* SW-846: Test methods for evaluating solid waste, physical/chemical methods: Washington, D.C., U.S. Environmental Protection Agency Office of Solid Waste, p. 3052-1–3052-20.

Weider, R. K., M. N. Linton, and K. P. Heston, 1990, Laboratory mesocosm studies of Fe, Al, Mn, Ca and Mg dynamics in wetlands exposed to synthetic acid coal mine drainage: Water Air and Soil Pollution, v. 51, p. 181–196.